

Supplement

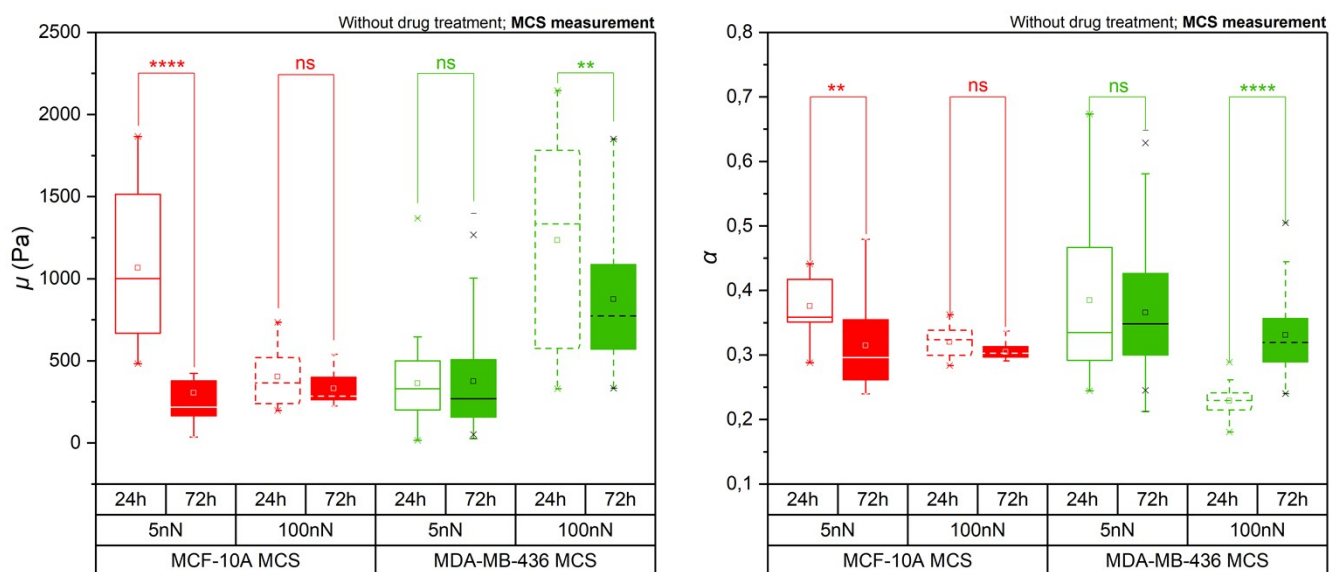


Fig. S1. Collective behaviors (contractility-based TST and shape-induced cell unjamming) tend to vanish over time. Time effect (24 hours culturing time, *open boxes*; 72 hours culturing time, *filled boxes*) of determining the surface (5nN, *solid outline*) and bulk (100nN, *dash outline*) mechanics of MCF-10A MCS (red) and MDA-MB-436 MCS (green), described by FE model parameters μ (left, a stiffness parameter) and α (right, a dimensionless fluidity parameter) [N=14 spheroids (10A, 24h, 5/100nN); N=16 (10A, 72h, 5/100nN); N=24 (436, 24h, 5nN); N=30 (436, 24h, 100nN) ; N=14 (436, 72h, 5N); N=33 (436, 72h, 100nN)]. For all conditions, without drug treatment, **** $p < 0.0001$, *** $p < 0.001$, ** $p < 0.01$, * $p < 0.05$, $p > 0.05$ non-significant by Welch's *t*-test.

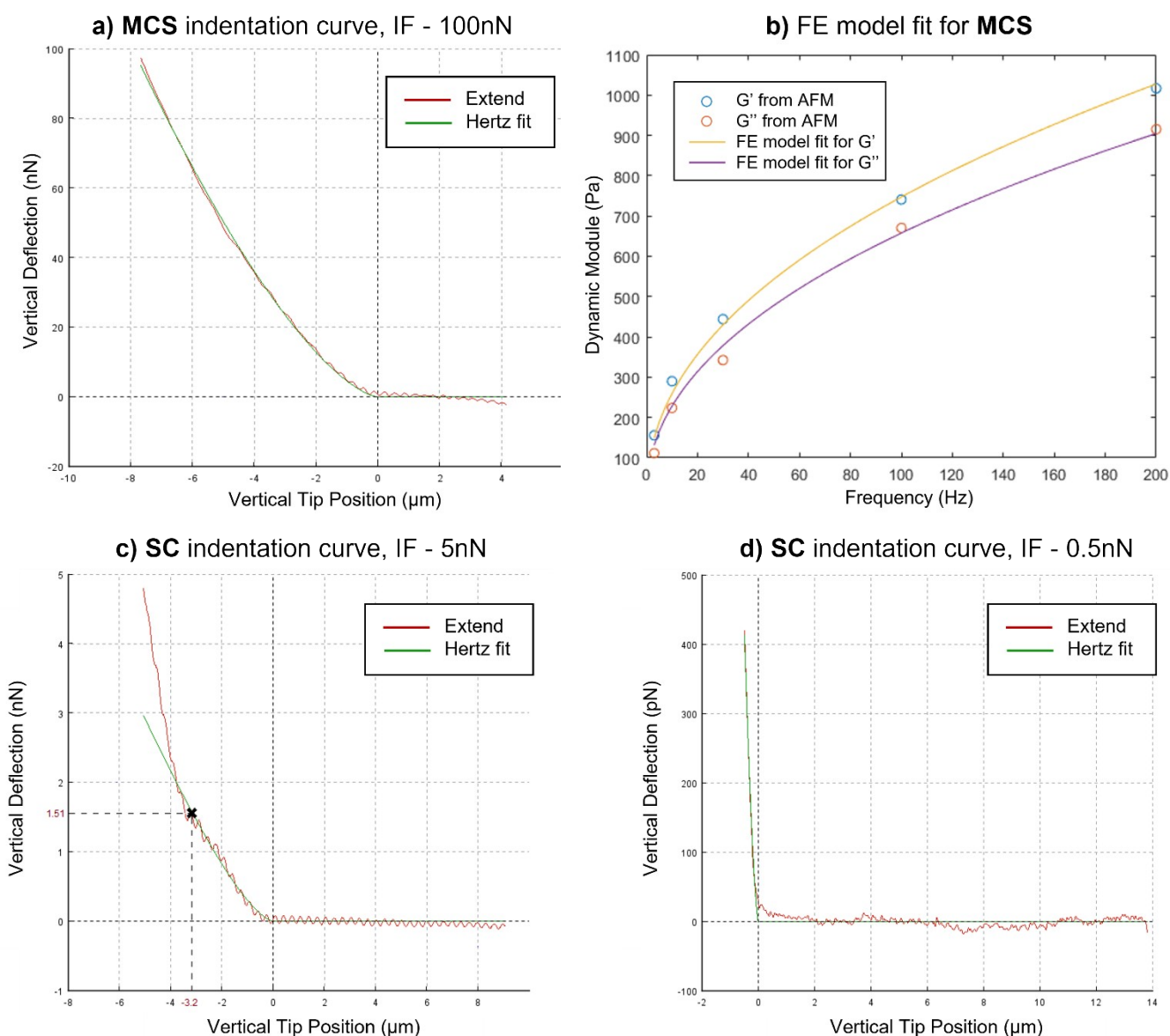


Fig. S2. An example to illustrate the fitting quality of chosen models. **a, c, d)** Hertz model was fitted to an extend force-indentation curve from AFM, extend data curves are in red and fit curves are in green. **a)** An indentation of $\sim 8 \mu\text{m}$ was performed on a $\sim 100 \mu\text{m}$ diameter MTS, the perfect alignment of Hertz fit indicates the indentation depth is still within the limits of the linear Hertz model. **b)** Fractional element model was fitted to the G' and G'' values of an AFM measurement. The G' and G'' were acquired by a built-in JPK data processing program using a sine fit to a frequency-dependent modulation segment. This step allows us to acquire a monotonic increase in storage and loss modulus over the full frequency range based on only two parameters: μ (left, a stiffness parameter) and α (right, a dimensionless fluidity parameter). **c)** The initial experiments were done using 5nN to align the loading force of the spheroids surface, where unfortunately the substrate effect is dominating the results (the indentation depth over $\sim 3 \mu\text{m}$). Hence a smaller IF of 0.5 nN was chosen to avoid such effect, **d)** shows an example of a perfect linear Hertz fit, such force (0.5nN) was used for the SC experiments in this study. Illustration curves here are from MDA-MB-436 MTS or SC, 24 hours culture time.

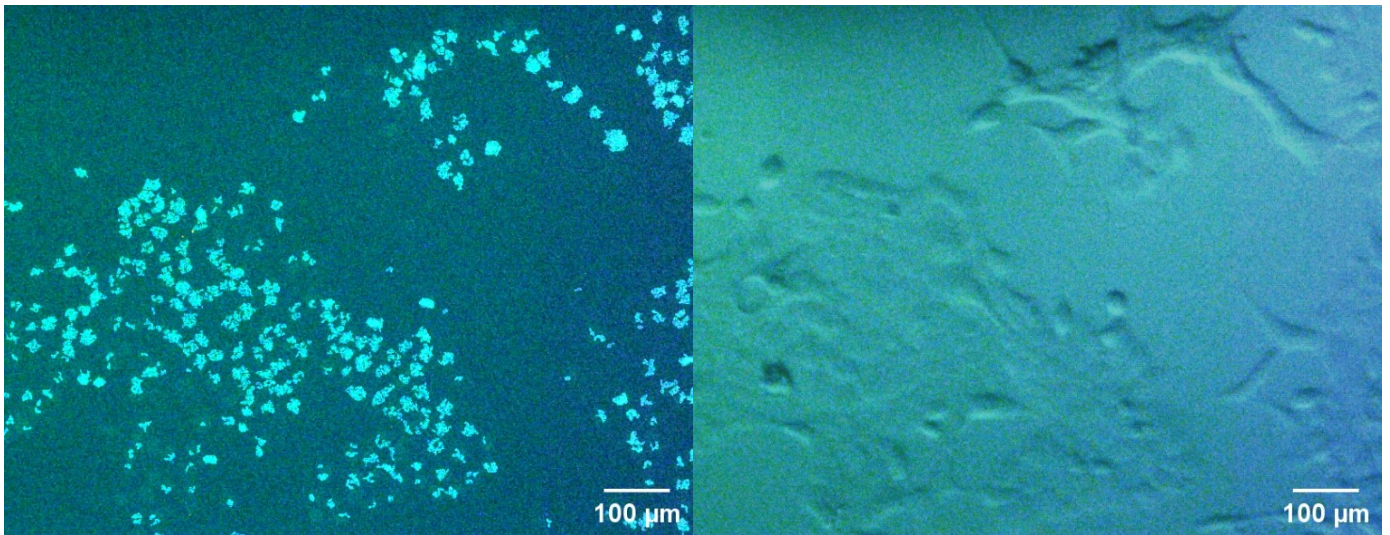


Fig. S3. Simultaneous fluorescence imaging on AFM while probing cell nuclei. The fluorescence image (left) and the bright field contrast image (right) of MCF-10A monolayers in the same field of view taken by AFM, local contrast enhanced with mask using ImageJ⁷⁶. Scale bar, 100 μm .

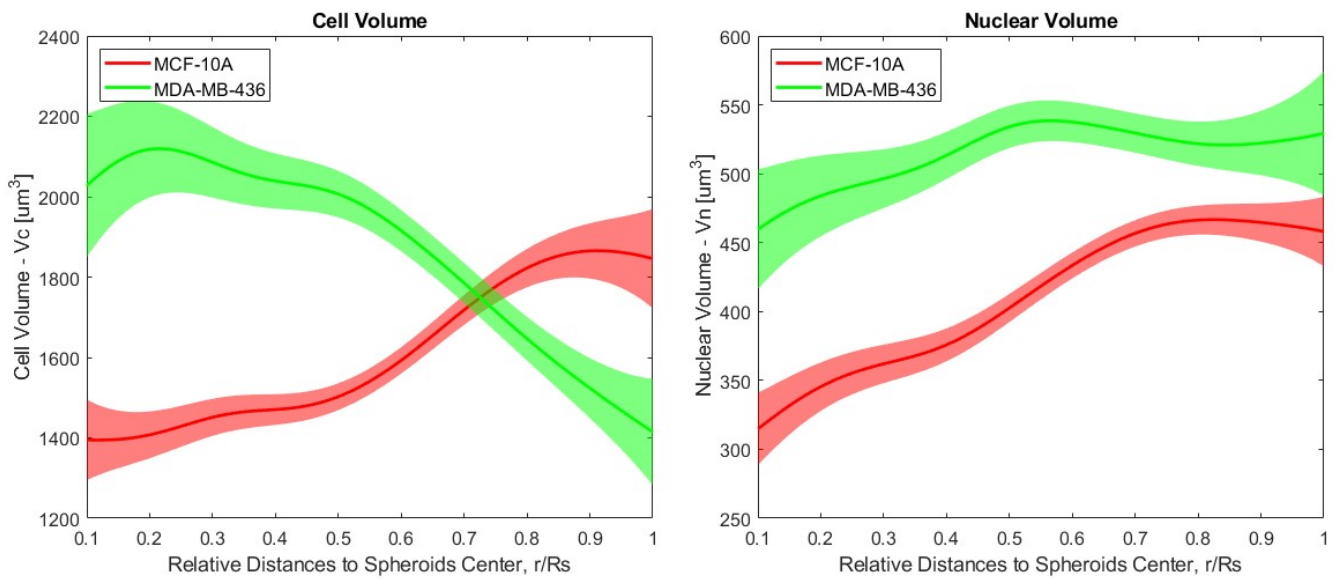


Fig. S4. The cancerous mesenchymal MDA-MB-436 cells contain larger nuclei than the healthy epithelial MCF-10A cells in MCS. Radial distribution of 3D cell volume V_c (left) and nuclear volume V_n (right) in MSCs, shaded areas are confidence intervals of moving bins $\text{FWHM} = 0.1R_s$ for $p = 0.05$ (r – the distance of each cell to the spheroid center, R_s – radius of the spheroid). MDA-MB-436 cells have in general larger nuclei and smaller cell volume on the surface of the spheroids, which agrees with our previous findings⁴.

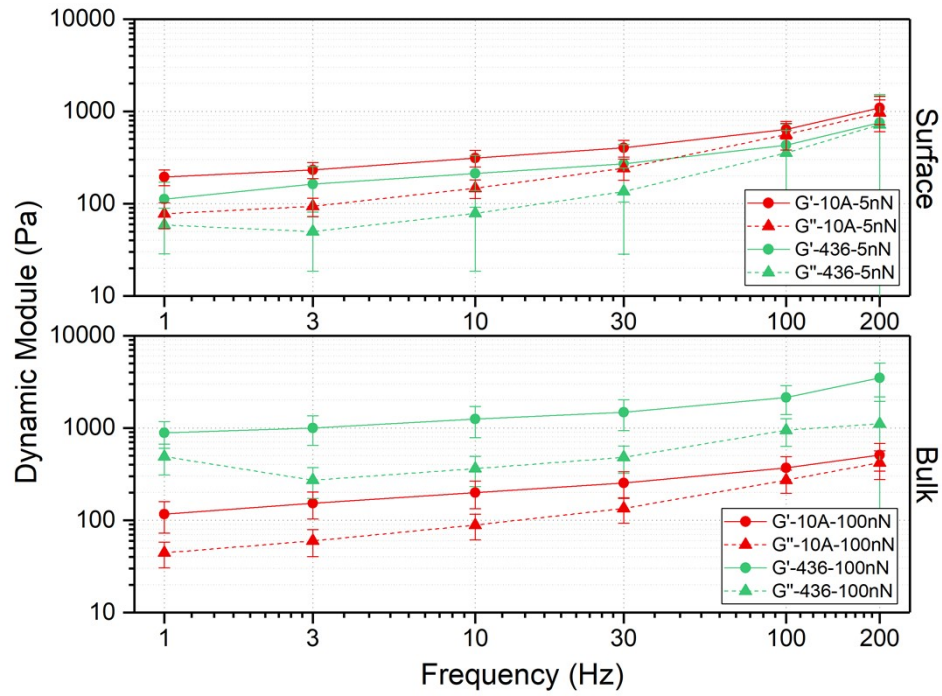


Fig. S5. Frequency-dependent power law behavior is observed for both type of MCS. Log-log plot of G' (solid line) and G'' (dash line) of MCF-10A MCS (red) and MDA-MB-436 MCS (green) with indentation force of 5nN (up, represents MCS surface) and 100nN (bottom, represents MCS bulk).

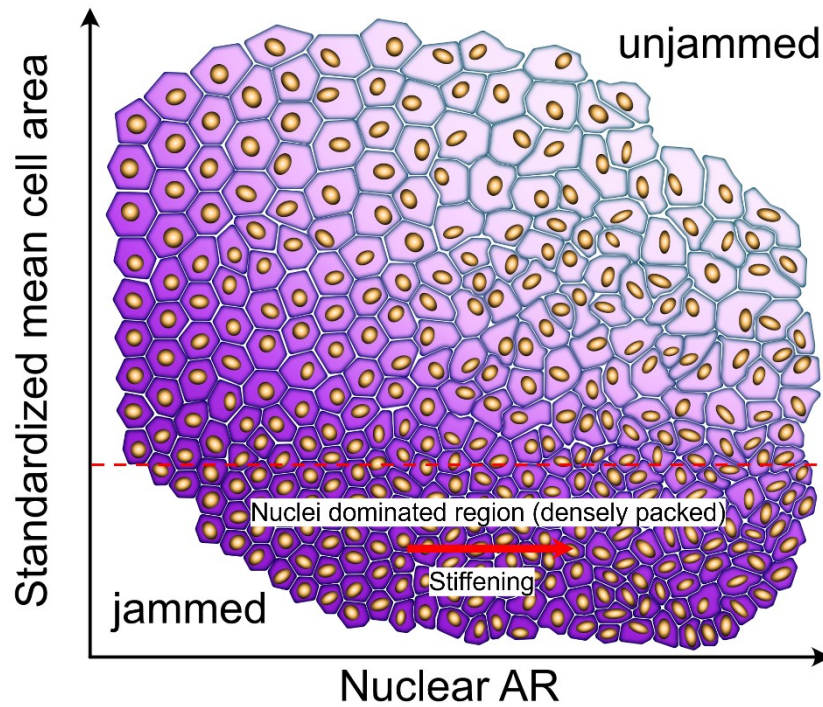


Fig. S6. State diagram of breast cancer cell unjamming readapted from Gottheil et al.³ Nuclei are marked in yellow, while cells are represented with a color gradient ranging from purple for jammed state to pink for unjammed state. Below the red dash line, cell area is small enough to let nuclei dominate the whole cell mechanics. With our finding from Fig.2, we know that with larger nuclear AR, a stiffer cell behavior was expected. Noted that it doesn't mean cell stiffening does not happen above the dash line. It simply means the stiffening from nuclear elongation will be less pronounced compared to the densely packed region.